Locking of ENSO and the Annual Cycle

Observations

- ENSO composite
- Coupling of ENSO and Annual Cycle

Hypotheses

- Annual ENSO
- Modulation of ENSO in the Delayed Oscillator
- Western Pacific ENSO turnabout

References

Rasmusson, E. M., T. H. Carpenter, MWR, 110, 354-384, 1982

Tozuka, T., T. Yamagata, JPO, 33, 1564-1578, 2003

Tziperman, E, M. A. Cane, S. E. Zebiak, Y. Xue, B. Blumenthal, J. Clim., 11, 2191-2199, 1998

Wang, B., R. Wu, R. Lukas, S. An, Dynamics of Atmospheric and Oceanic Circulation and Climate, 552-578, April 2001

Wang, X. L., JAS, 51, 115-1136, 1994

ENSO Composites

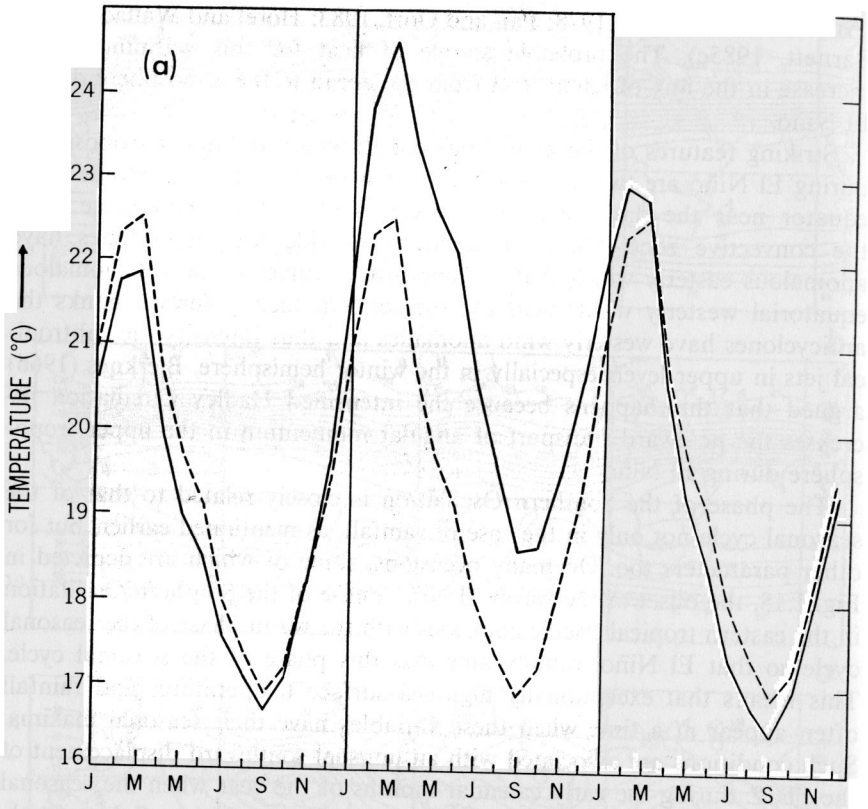

Figure 1.18. (a) The seasonal sea surface temperature changes (dashed line) and the changes during a typical El Niño episode as measured along a ship track 100 km off the coast of South America between 3°S and 12°S. (b) Sea surface temperature departures from the seasonal cycle, along the track mentioned in (a), during El Niño episodes in 1951, 1953, 1957, 1963, 1965, 1969, and 1972. The figure also shows variations during the preceding and following years. The solid line in (a) is obtained by averaging the curves in (b). [From Rasmusson and Carpenter (1982a).] (*Figure continues*)

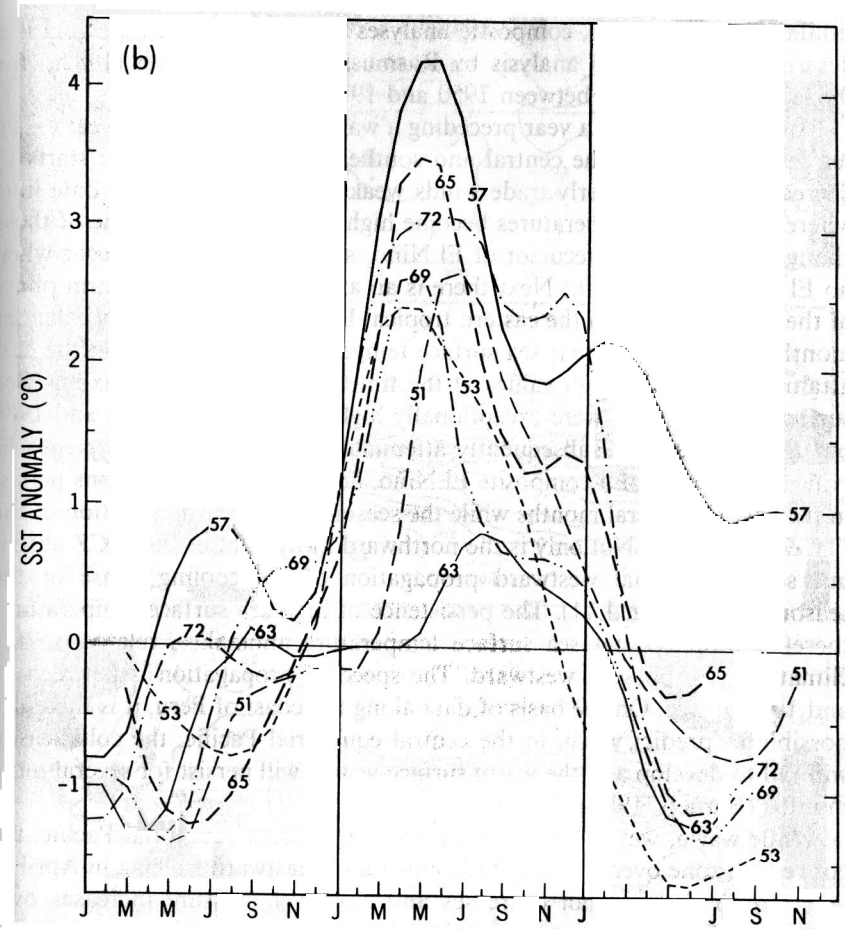

Figure 1.18 (*Continued*)

Philander 1990, Rasmusson and Carpenter 1982

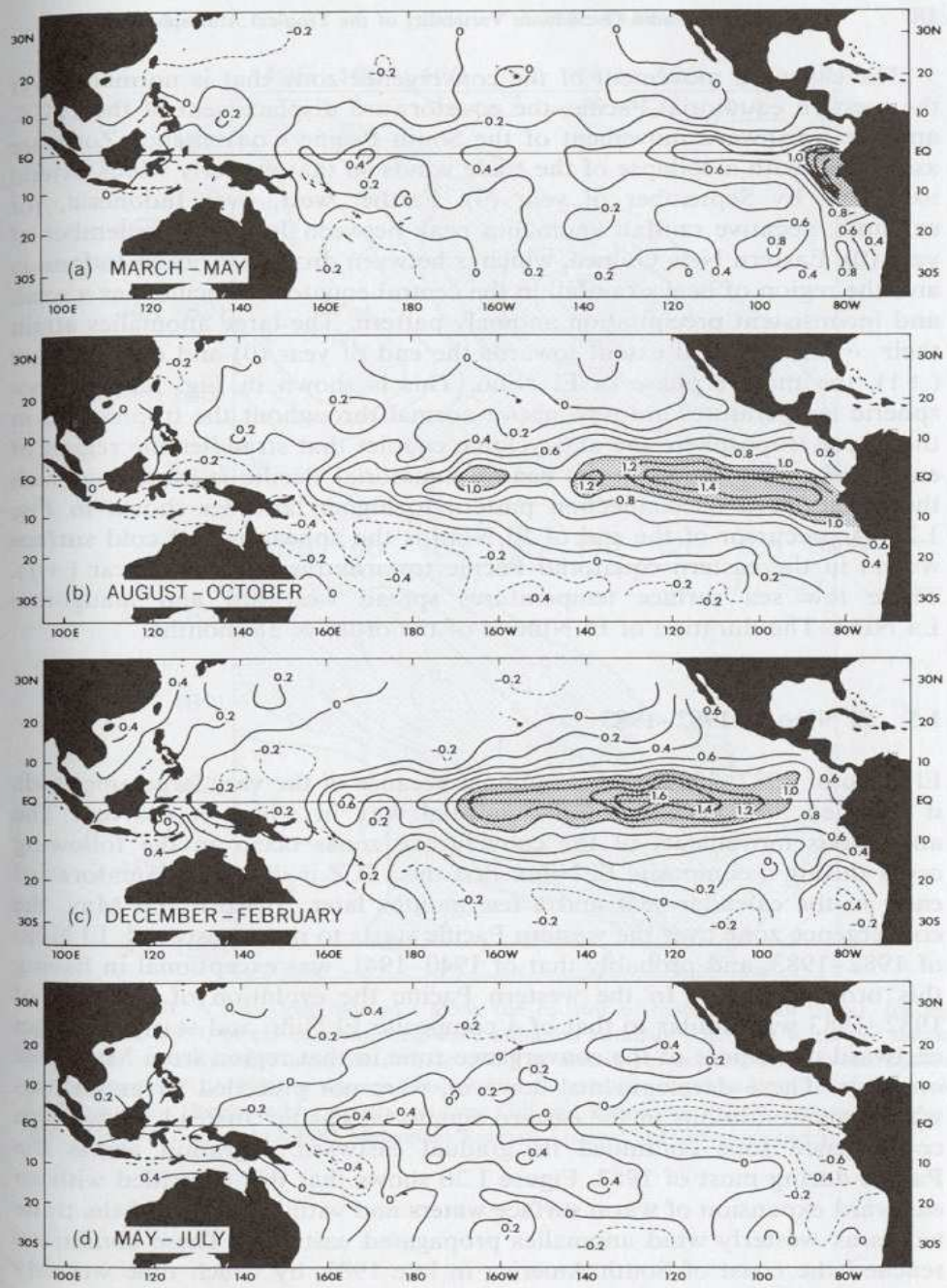

Figure 1.19. Sea surface temperature anomalies (in °C) during a typical El Niño obtained by averaging data for the episodes between 1950 and 1973. (a) March to May after the onset, (b) the following August to October, (c) the following December to February, and (d) May to July more than a year after the onset. [From Rasmusson and Carpenter (1982a).]

Philander 1990, Rasmusson and Carpenter 1982

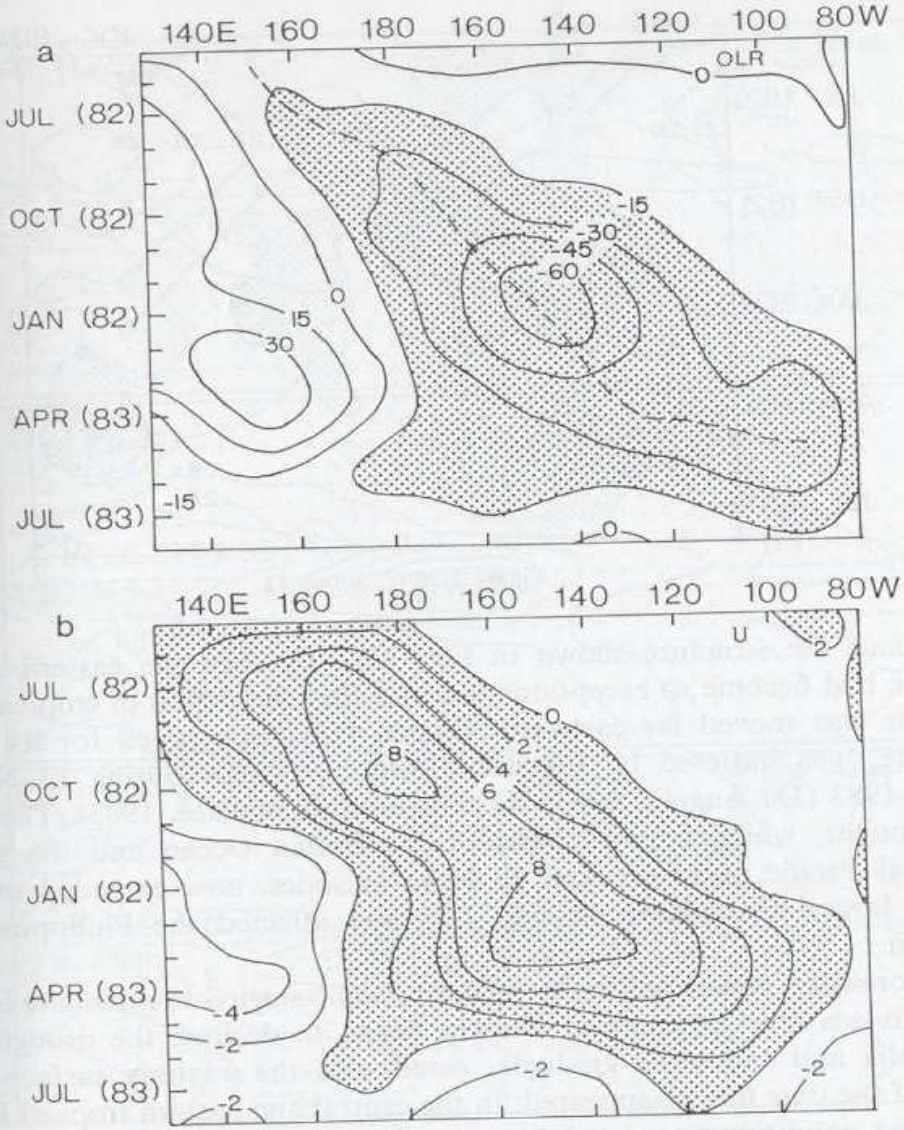

Figure 1.20. A time–longitude plot along the equator of monthly mean values, for the period 1982–1983, of (a) outgoing long-wave radiation anomaly (OLR) in watts per square meter, (b) westerly wind anomaly (5°S to 5°N) in meters per second, and (c) sea surface temperature (4°S to 4°N) in degrees Celsius. The dashed lines in (a) and (c) follow the peak OLR anomaly. [Reprinted by permission from Gill and Rasmusson (1983). *Nature (London)* **305**, 229–234. Copyright ©1983 Macmillan Journals Limited.] (*Figure continues.*)

Philander 1990

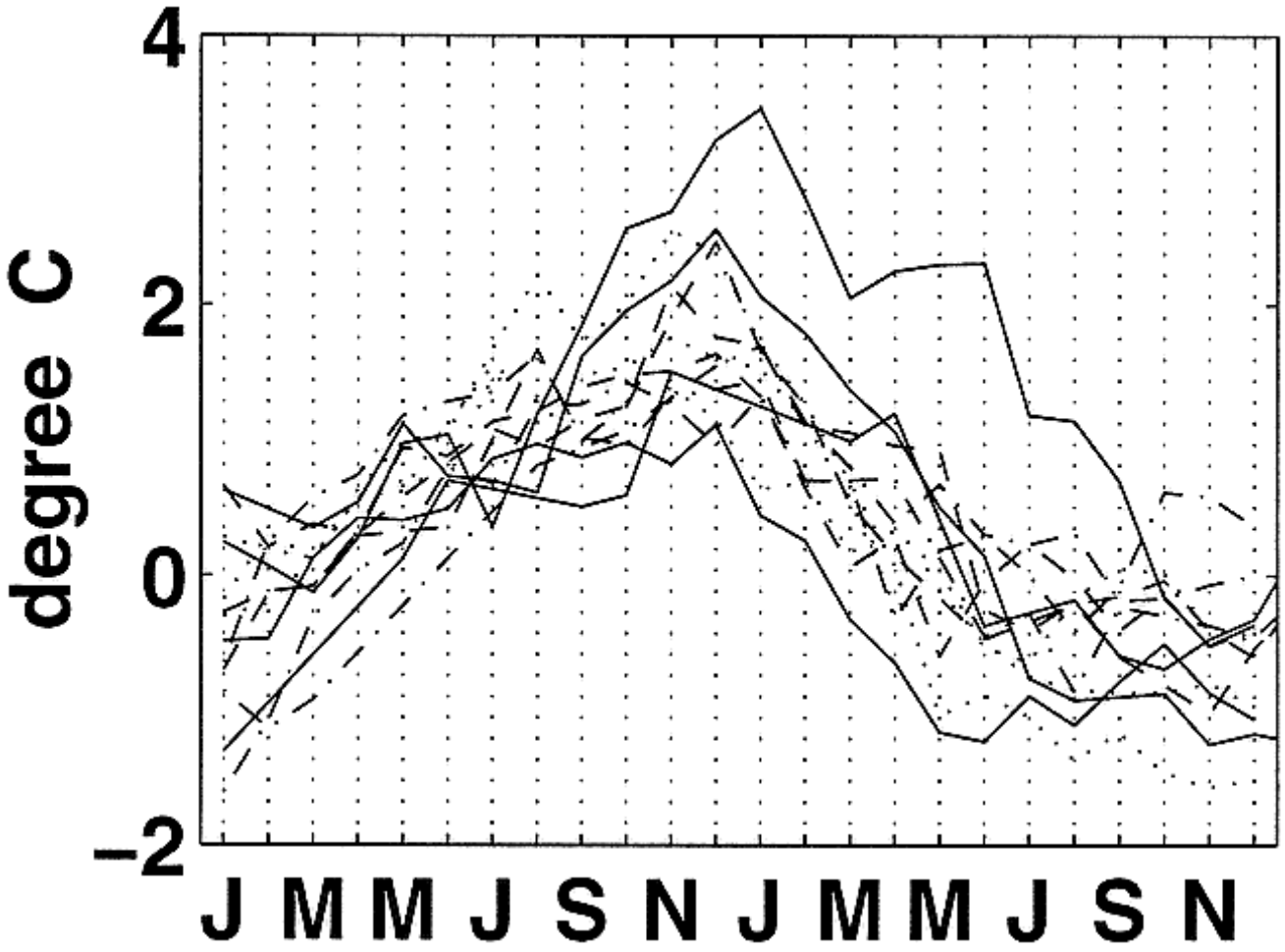

Tziperman et al. 1998

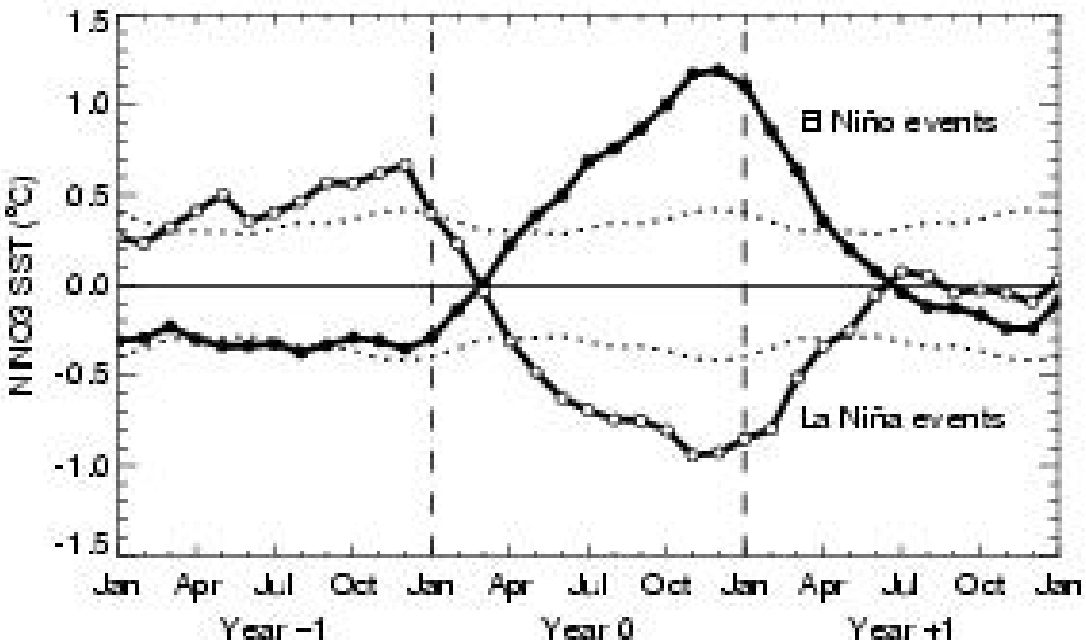

Figure 3. Composite of the 29 El Niño events and 22 La Niña events occuring between 1877-1995, as defined by Kiladis and Diaz (1989). The composite is the mean of monthly SST anomalies for all warm events (solid dots) or cold events (open dots). Year 0's are defined as in Rasmusson and Carpenter (1982). Dotted lines mark the 95% confidence levels for a mean of 22 points taken from a population with the monthly-varying standard deviations of the entire NINO3 SST time series.

Torrence and Webster 1998

Coupling of ENSO and the Annual Cycle

Coupling of ENSO and annual cycle

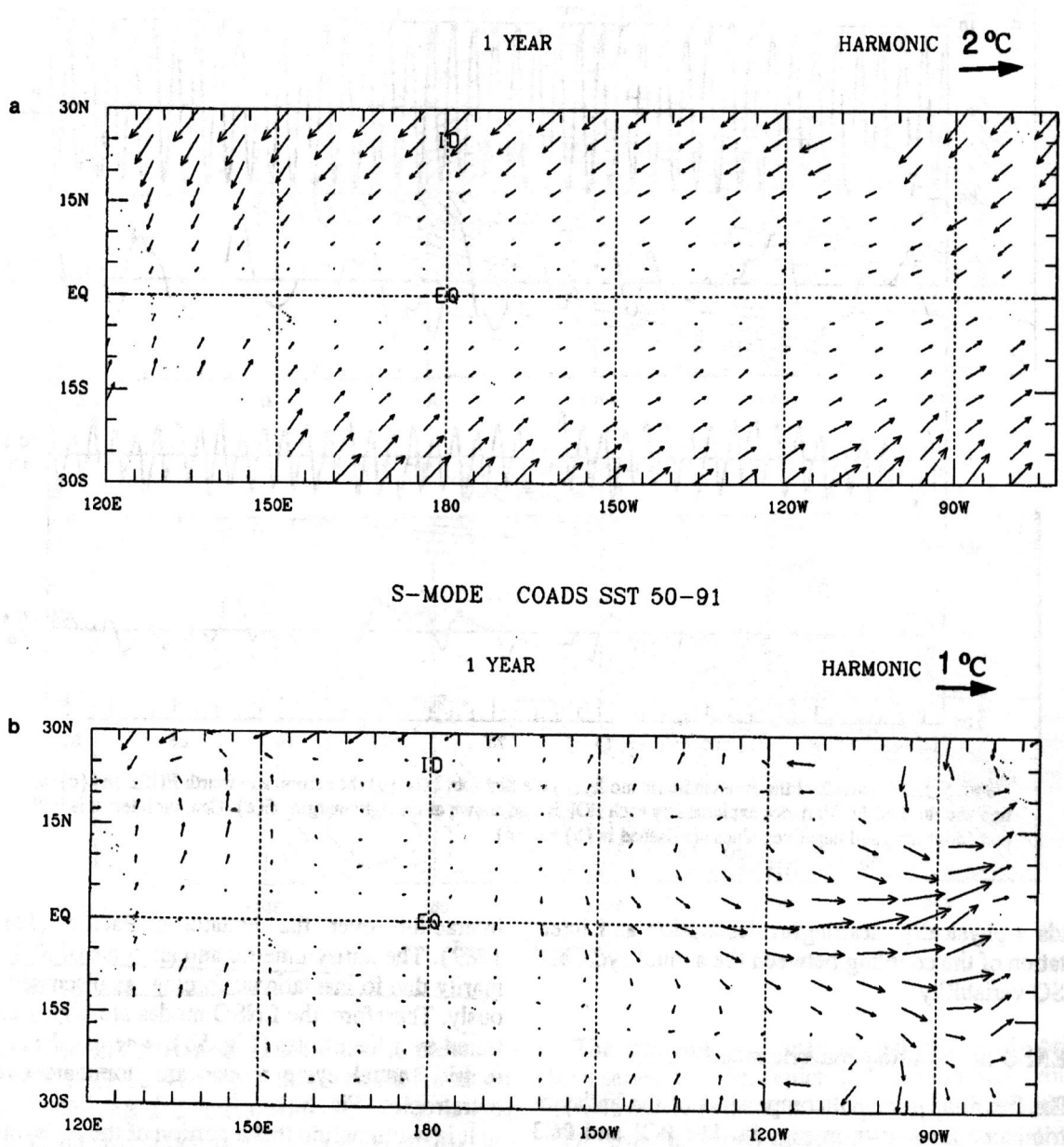

FIG. 4. Annual harmonic of the antisymmetric annual cycle (a) and the symmetric annual cycle (b). Amplitudes of the annual cycle are indicated by lengths of the arrows according to the scale in the figure. An arrow pointing north indicates a maximum of SST on 1 January; to the east a maximum on 1 April, etc.

Wang splits the mean annual cycle into equatorial symmetric and antisymmetric parts. He then estimates the EOFs of the sum of interannual anomalies with either the symmetric or the antisymmetric parts of the seasonal cycle. This indicates that only the equatorial symmetric part interacts with ENSO.

Wang 1994

Principal components 1-4 of sum of equatorial symmetric seasonal cycle and interannual anomalies. Note the distinct differences in character of EOF 1, 3 compared to EOF 2, 4 ....

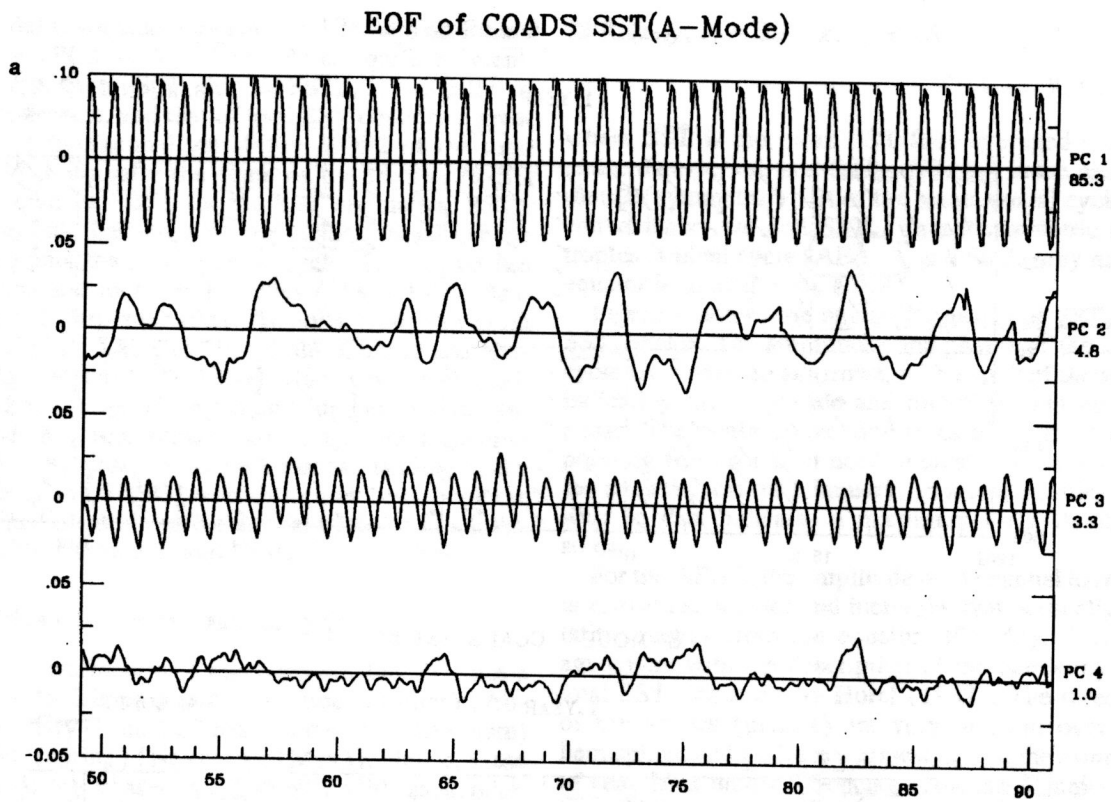

FIG. 5. EOF analysis of the antisymmetric mode, (a) the first four PCs, (b) the second and fourth EOFs, and (c) the first and third EOFs. Variance explained by each EOF is also shown at the right margin of (a). Contour interval is 0.01 unit (arbitrary) and negative values are dashed in (b) and (c).

Wang 1994

... and EOF 1 and 3 recover the symmetric seasonal cycle, while EOF 2 and 4 capture the interannual anomalies.

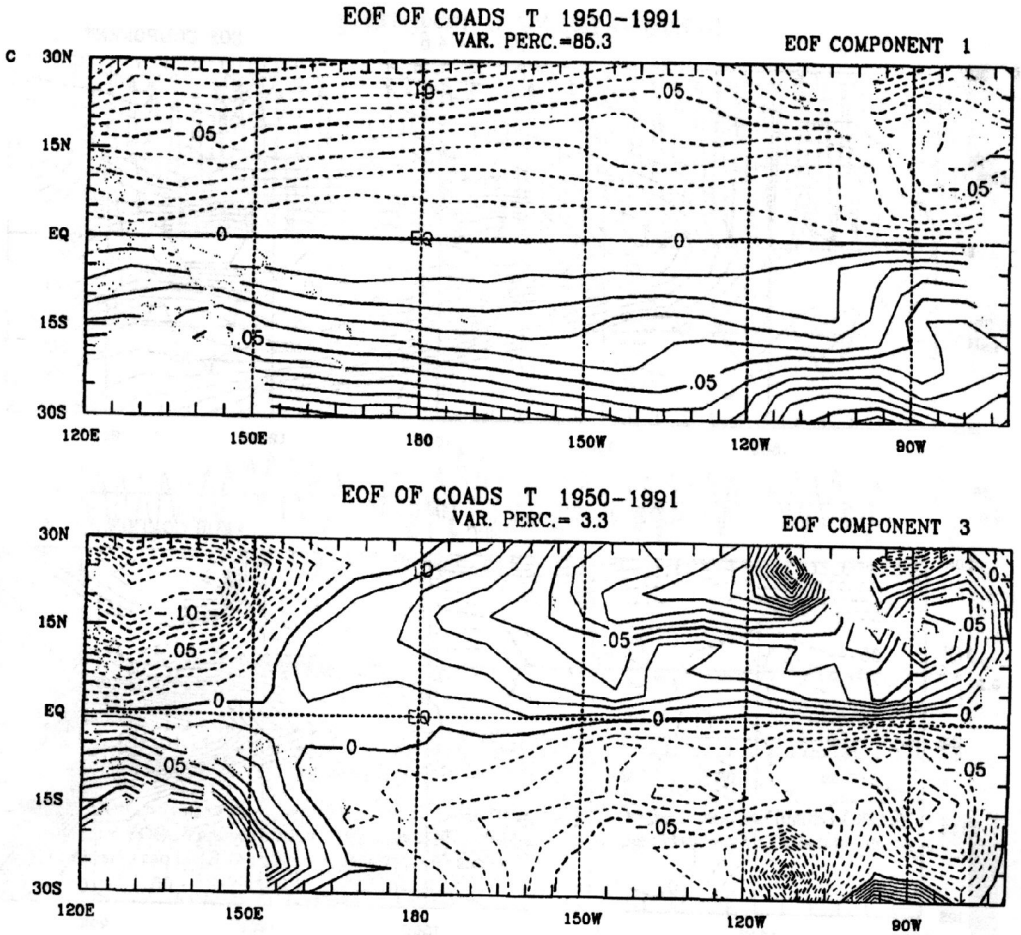

FIG. 5 (*Continued*)

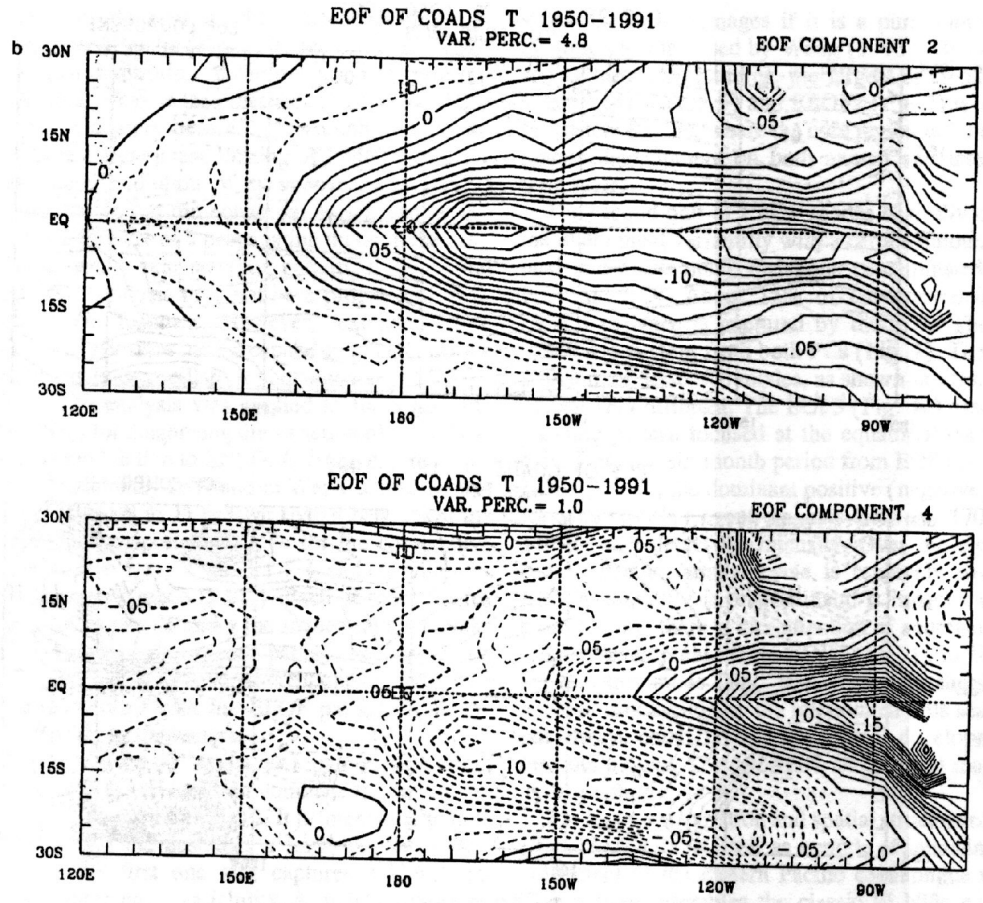

FIG. 5 (*Continued*)

EOF 1, 3

EOF 2, 4

Wang 1994

In contrast, the EOFs of symmetric annual cycle and interannual anomalies can not be separated.

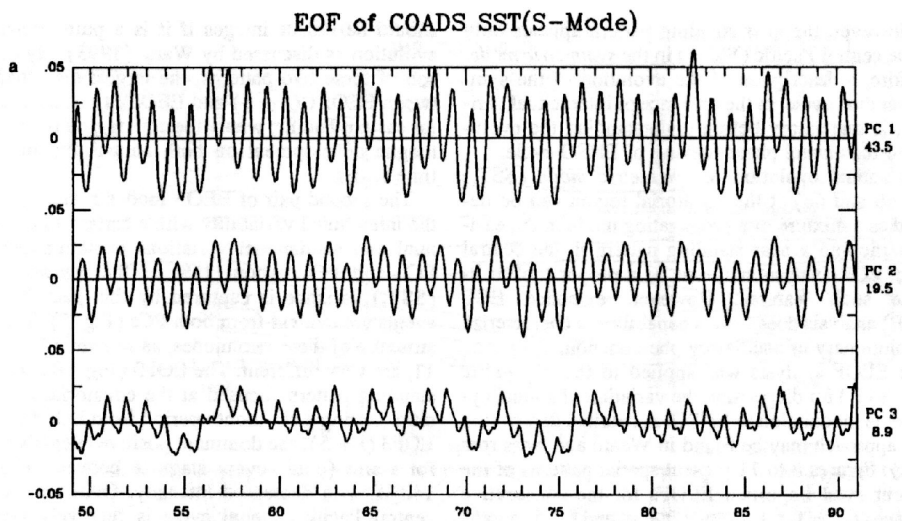

FIG. 6. EOF analysis of symmetric mode, (a) the first three PCs, (b) the first three EOFs, and (c) the mean annual cycle of the PCs in (a). Variance explained by each EOF is also shown at the right margin of (a). Contour interval is 0.01 unit (arbitrary) and negative values are dashed in (b).

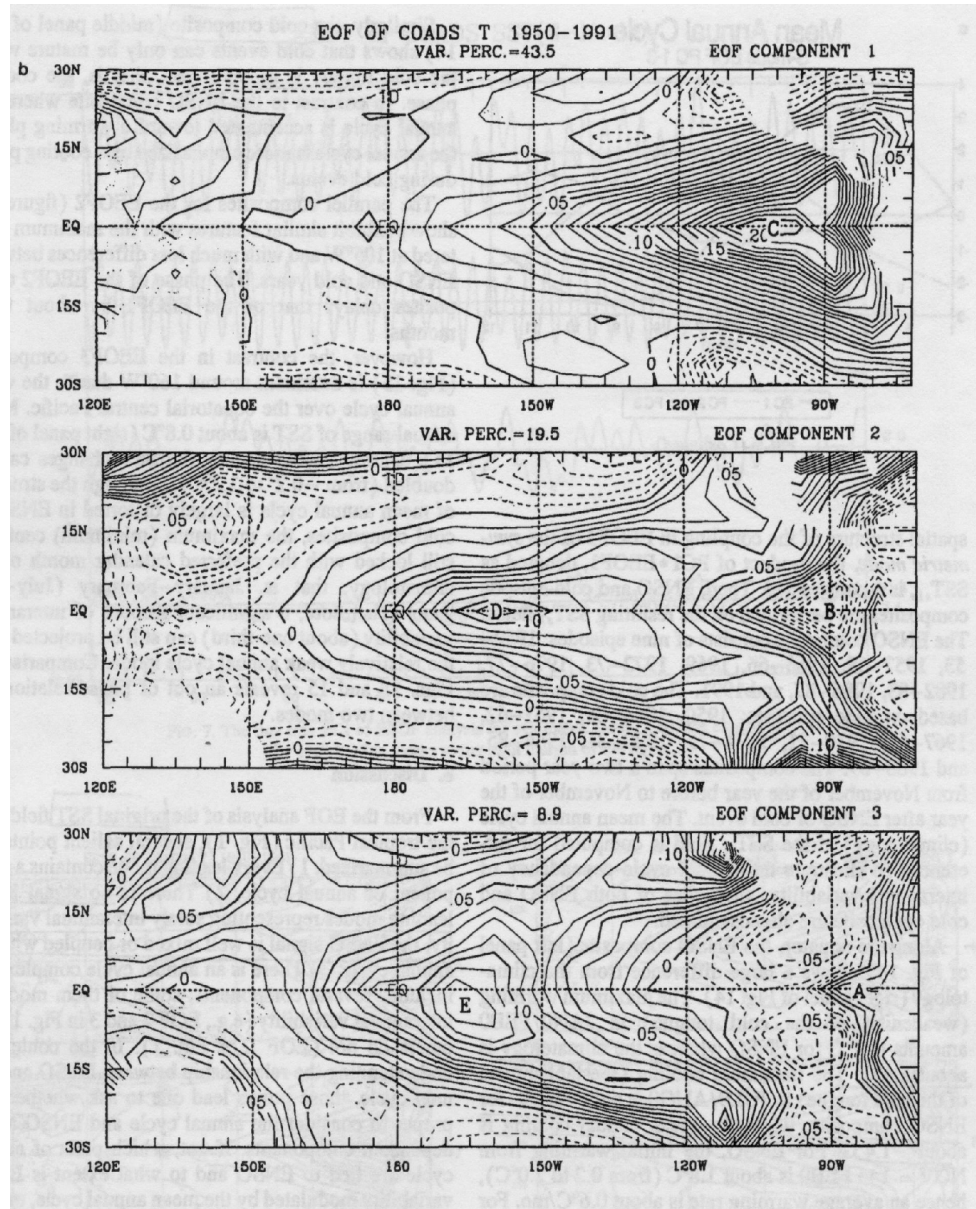

Wang 1994

Modulation of mixed layer depth in eastern Pacific by interannual forcing

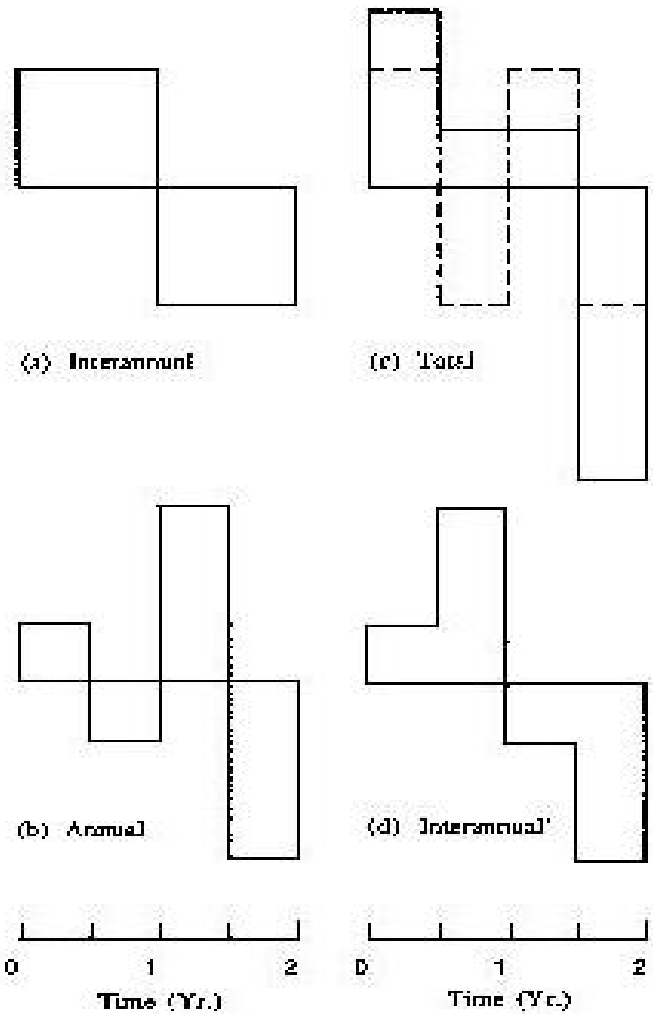

FIG. 9. Schematic illustrating how interannual anomalies of sea surface temperature are phase-locked to calendar seasons. (a) Interannual cycle in sea surface temperature or the thermocline depth, (b) annual cycle whose amplitude is modified by the interannual variation in the thermocline depth, (c) total SST deviation from the long-term annual-mean value and mean annual cycle (dashed line), and (d) SST deviation from the mean annual cycle.

$$\frac{dT}{dt} = \frac{Q}{H(1+h)}$$

seasonal forcing

mixed layer depth modulated by interannual anomalies

Note: this argument only works if the ENSO period is an integer multiple of the annual period.

Xie 1995

Annual ENSO

Tozuka and Yamagata explain the annual evolution in the equatorial region as resulting from a propagating coupled wave that extends the warm/cool conditions off S. America towards the west. ENSO, initiated in the west, is an eastward propagating anomaly, that deepens the thermocline in the central and eastern equatorial Pacific, and thereby modulates the annual cycle and leads to a weaker cold season and warmer warm season.

Annual Cycle 72-73 ENSO 82-83 ENSO

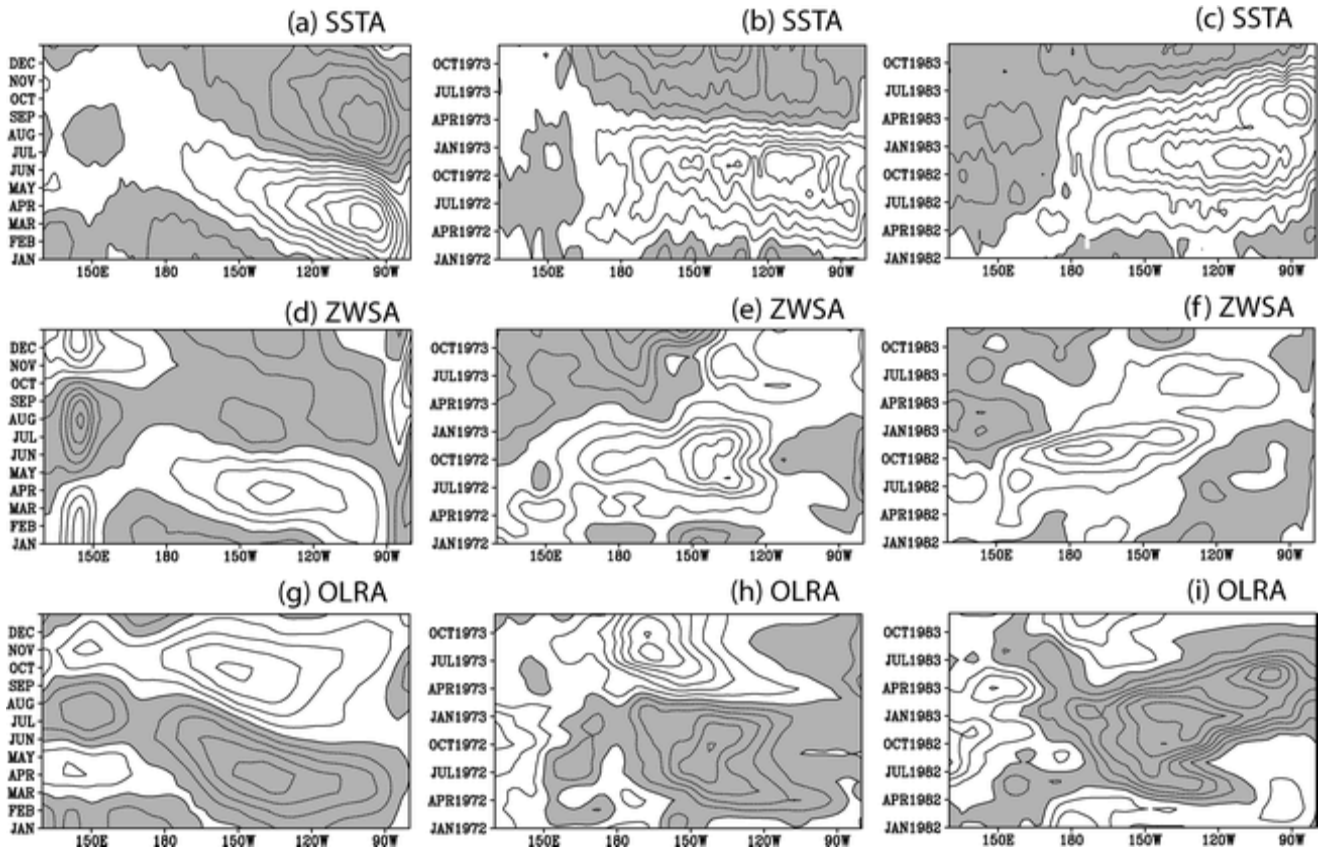

Tozuka and Yamagata 2003

Schematic of Annual ENSO: westward propagating coupled anomalies develop in in response to seasonal variations off S. America

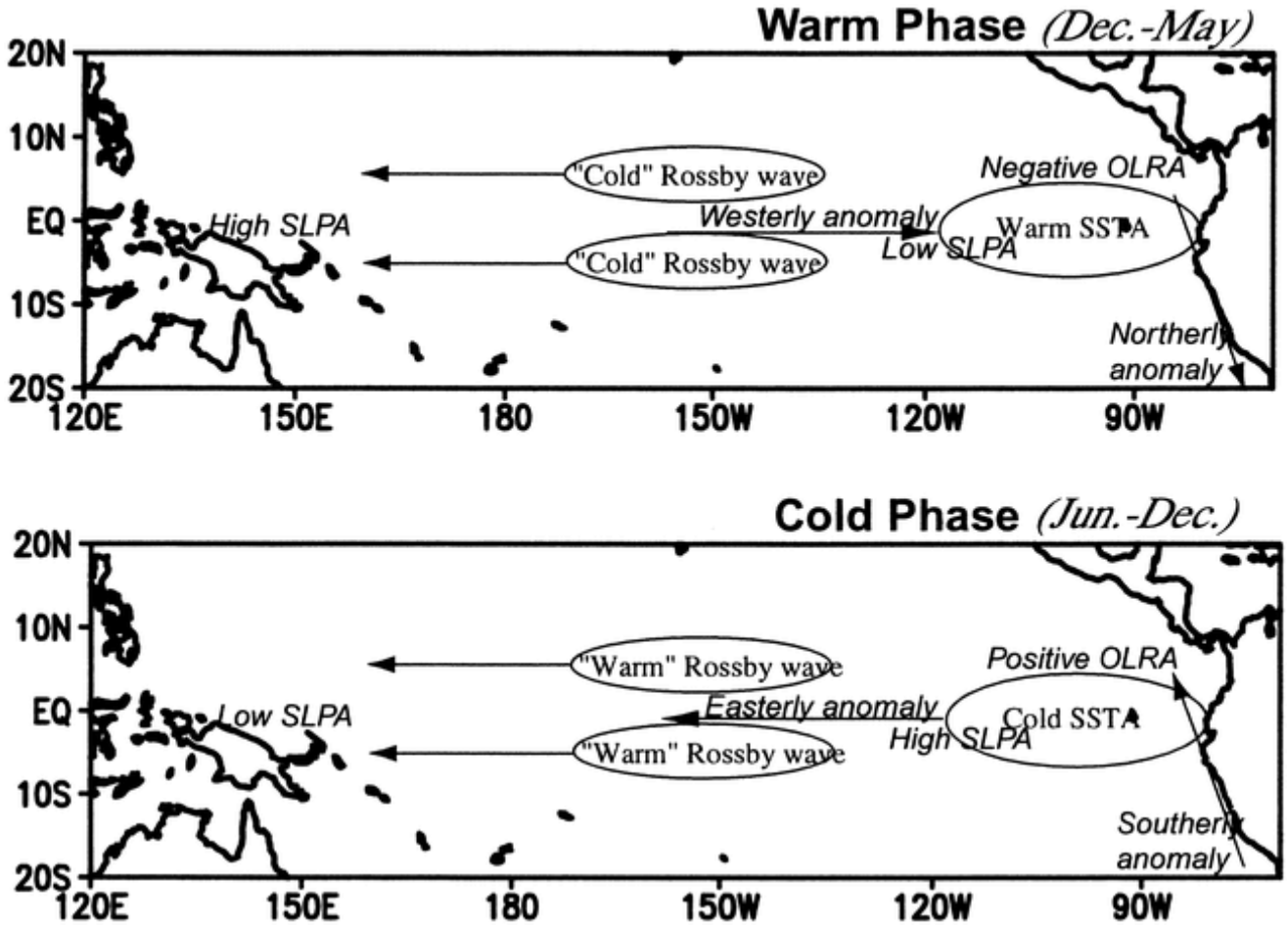

Tozuka and Yamagata 2003

Interannual Variability

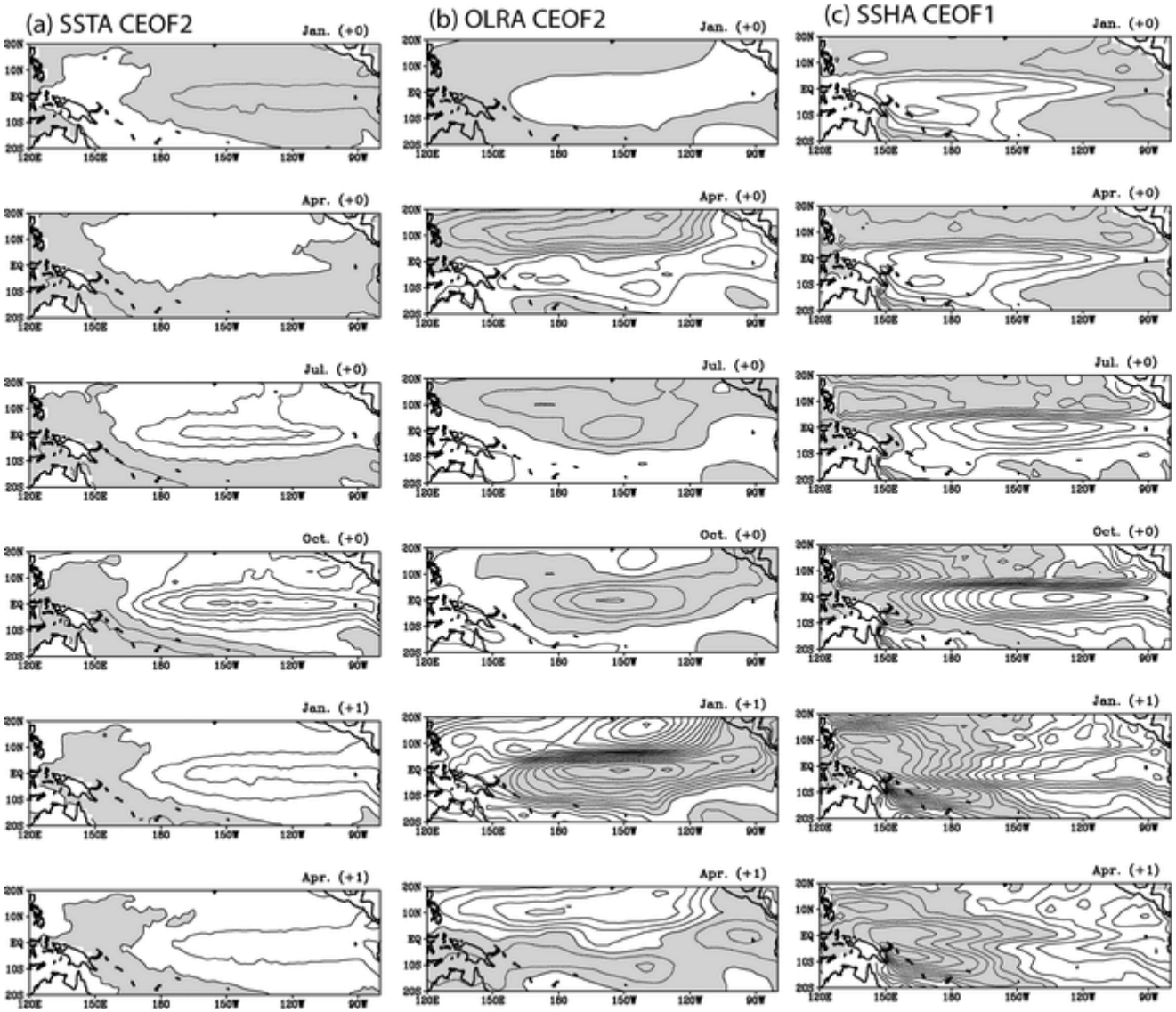

El Nino is associated with a deep thermocline in the east ...

Tozuka and Yamagata 2003

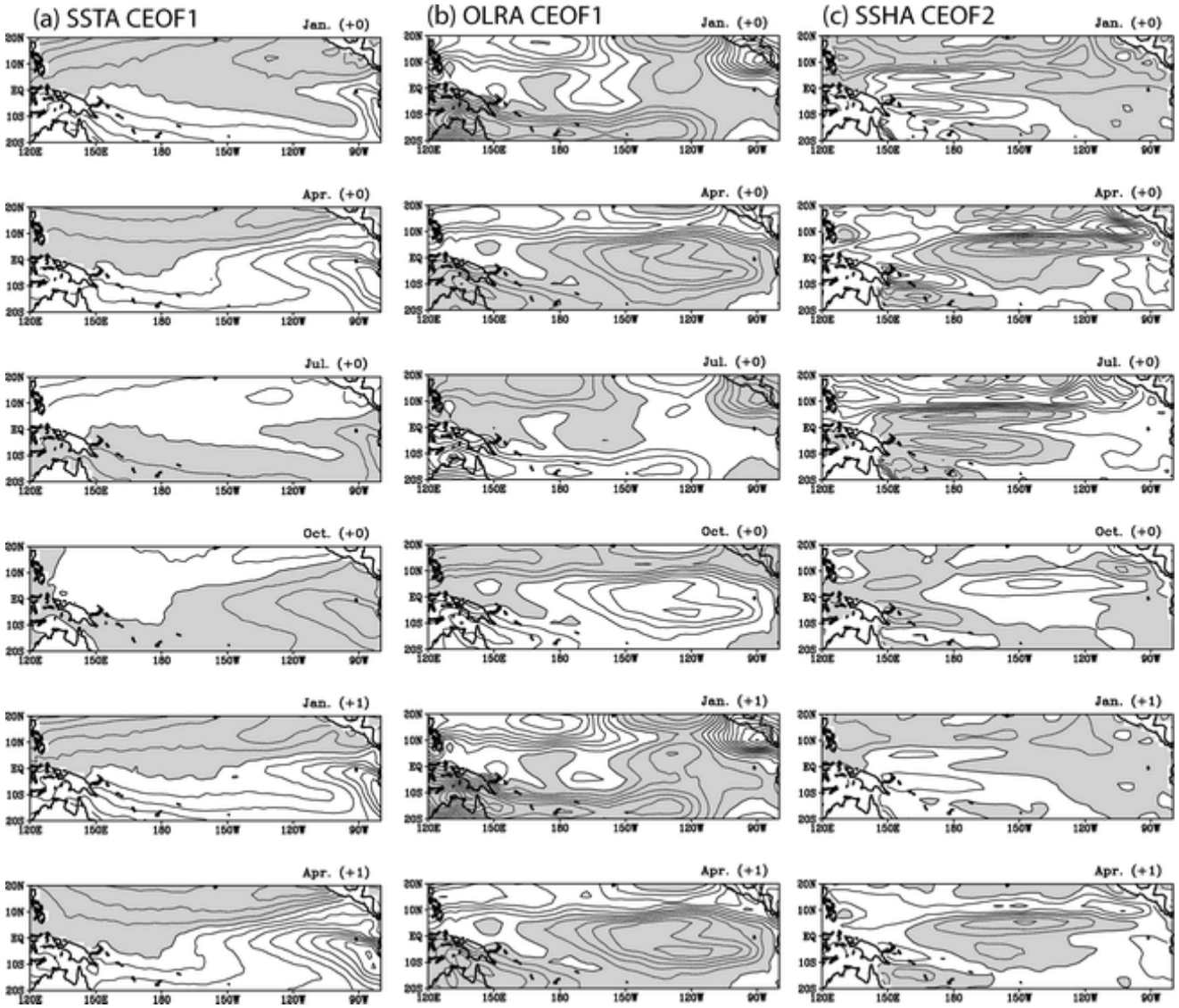

.. that then leads to an enhance seasonal warming there.

Tozuka and Yamagata 2003

Nonlinear thermocline temperature

Delayed oscillator equation with annual cycle forcing; ENSO modeled as a low-order chaotic process driven by the annual cycle.

$$\frac{dh(t)}{dt} = a\,A(h\{t-[L/(2C_K)]\})$$
$$-b\,A(h\{t-[L/C_K+L/(2C_R)]\})+c\cos(\omega_a t)$$

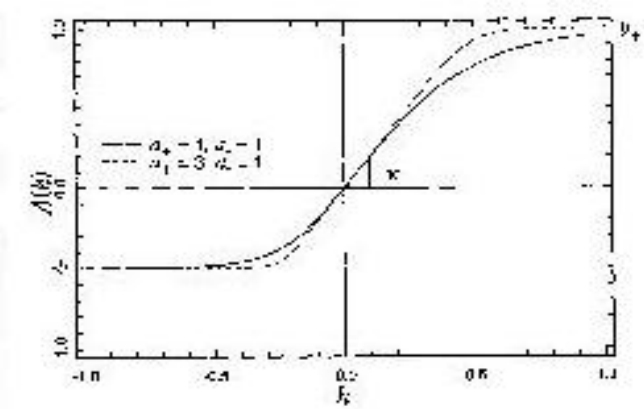

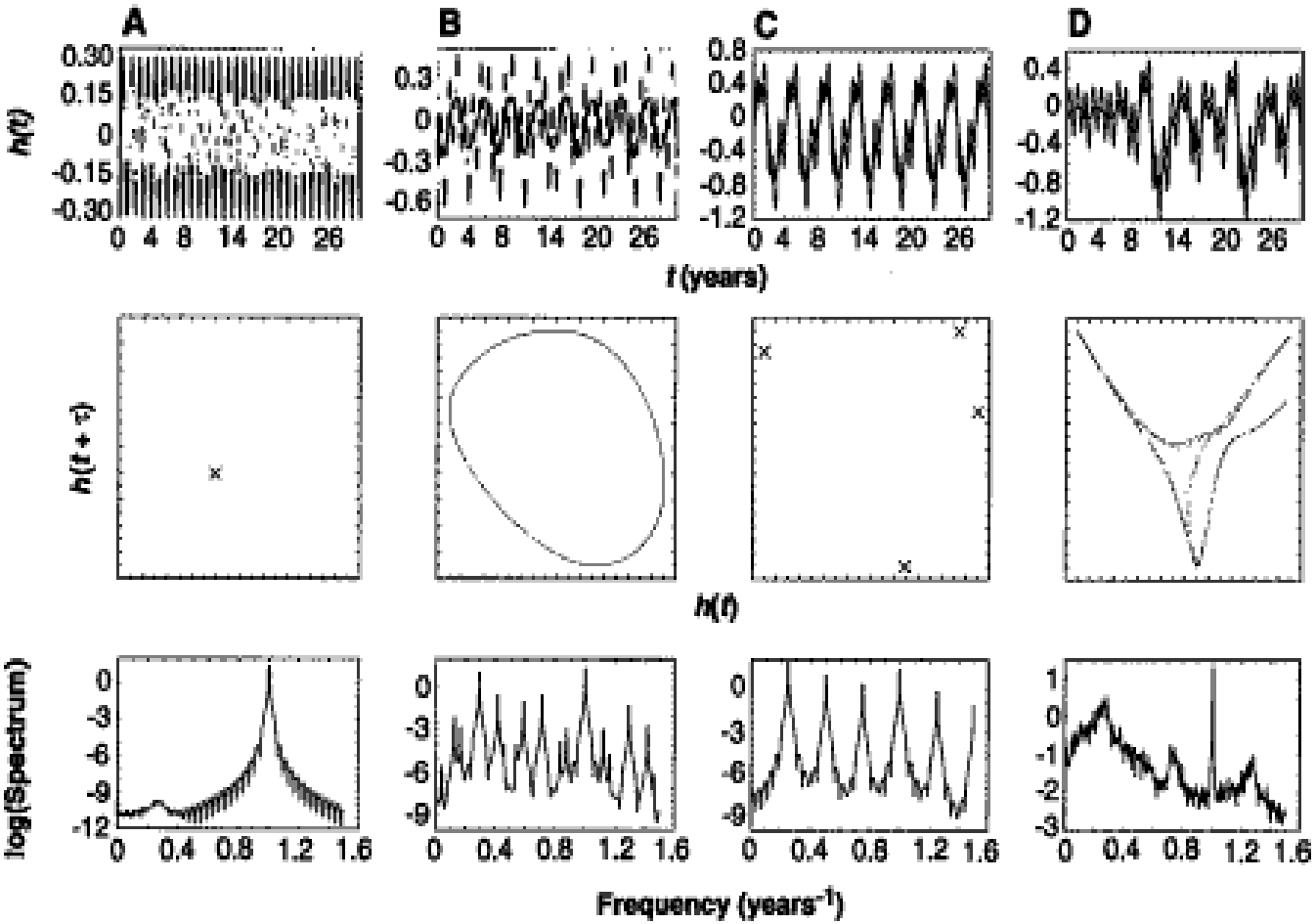

From left to right: increase nonlinearity of A(h), solution goes from a n oscillation at annual period, irregular oscillations, mode locked and chaotic. Mode locked and chaotic solution have maximum deviations in same 4 month of the calendar year. Small nonlinearity: quasi-periodic or mode-locked to a single nonlinear resonance. Higher nonlinearity: two or more mode locked solutions coexist. Tziperman et al. 1994

Nonlinearity of thermocline temperature and advection terms

Stripped down coupled model for equatorial ocean, including 'full' SST equation (mode), forced by annual cycle. Vary δ_S the importance of zonal and vertical advection leads to frequency-locked steps created by nonlinear resonance with the annual cycle. Behavior is also sensitive to coupling strength μ.

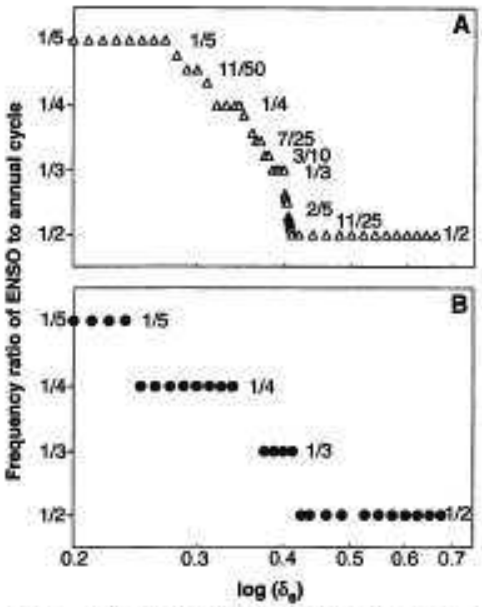

Fig. 1. Frequency ratio of the model El Niño oscillation to the annual cycle, as a function of a parameter, δ_s, that affects the inherent ENSO period. Another parameter, the coupling coefficient, μ, is changed to keep the El Niño cycle below its transition to chaos. Nonlinear frequency locking to the annual cycle creates a staircase of discrete steps at rational values of the frequency ratio. For instance, for a frequency ratio 1/4, the ENSO period is exactly 4 years, while for 3/10, a sequence of three El Niño cycles repeats every 10 years. (**A**) The approximate devil's staircase, slightly above the primary Hopf bifurcation where the ENSO mode goes unstable. All points shown correspond to rational frequency ratios (some labeled). (**B**) Frequency-locked solutions for slightly larger (by about 10%) values of μ, showing the rapid widening of the integer-period steps.

Devil's Staircase: inherent frequency of system locks onto a sequence of rational fractions of the external frequency, associated with the transition to chaos by the overlapping of these nonlinear resonances.

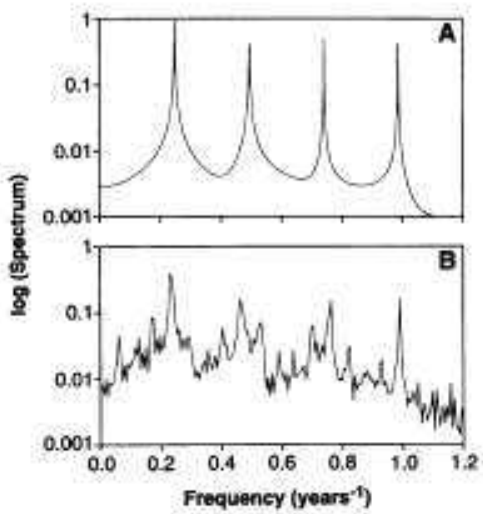

Fig. 2. Power spectra of eastern Pacific equatorial SST (averaged from 135°W to 90°W) from the last 500 years of two 520-year model integrations (bandwidth of 0.06 year^{-1}). (**A**) For a case of frequency locking to 4-year period. (**B**) For a case with a slightly higher value of the coupling parameter, μ, which exhibits chaotic behavior.

to the accuracy of El Niño forecasts. In our

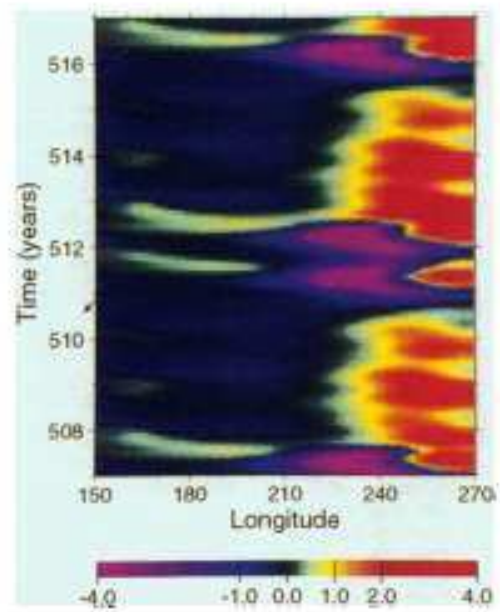

Fig. 3. Time-longitude plot of Pacific SST anomalies along the equator, for a typical 10-year interval from the model run corresponding to Fig. 2B.

Interaction of ENSO mode and annual cycle occur though upwelling and thermocline slope, and their response to seasonal wind stress forcing.

Jin et al. 1994

Seasonal modulation of the coupling strength in the ENSO in delayed oscillator

Kelvin wave, 1 month delay, positive feedback

$$\frac{dh}{dt} = b\,A[\kappa(t-\tau_1)\,h(t-\tau_1)] - c\,A[\kappa(t-\tau_2)\,h(t-\tau_2)] - d\,h(t)$$

Rossby wave, 6 month delay, negative feedback

Solution segment of the model

Coupling strength

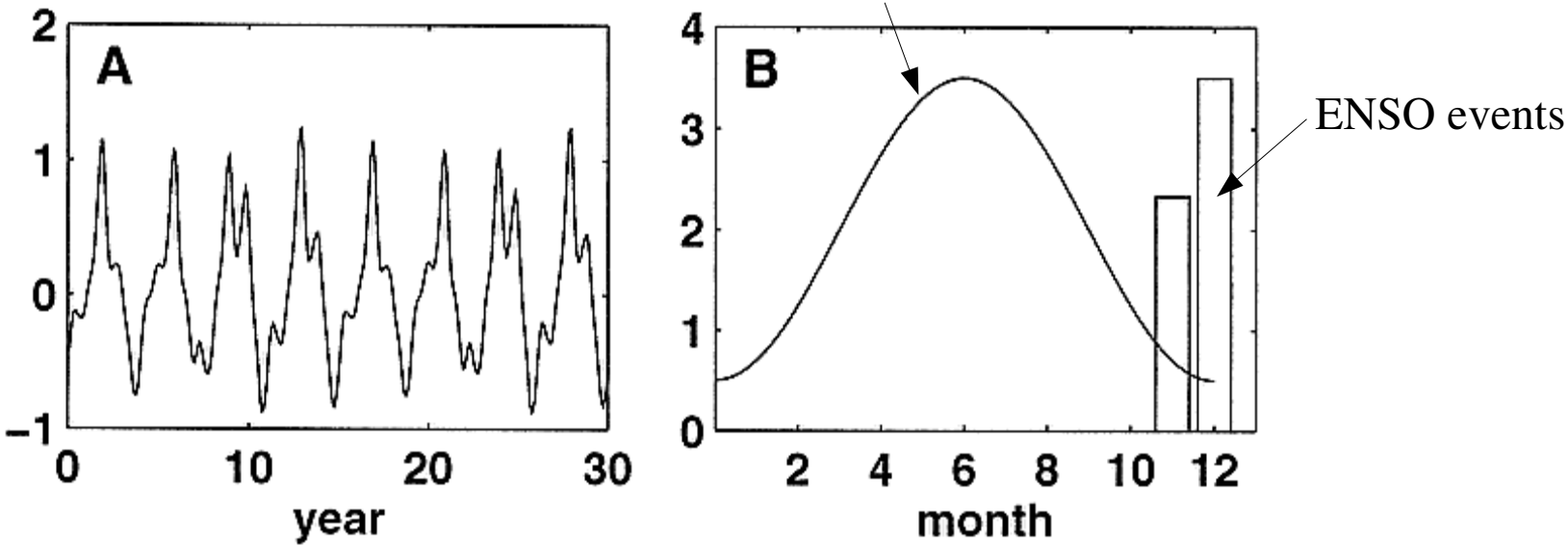

Coupling strength strongest during boreal spring and summer, and weakest during early winter due to: ITCZ close to equator, large mean horizontal SST gradients, shallow thermocline, strong winds, high SST and strong upwelling.

Tziperman et al. 1998

Why do ENSO perturbations peak when coupling is weakest?

Peak at dh/dt=0: this can only be achieved in winter, when the large Kelvin wave amplitude, multiplied by weak coupling, can balance the weak Rossby wave of 6 month prior, multiplied by a strong coupling.

The opposite phasing does not work: assume ENSO peaks in summer: the large Kelvin wave amplitude is multiplied by a strong coupling can not balance the weak Rossby wave amplitude of 6 month prior multiplied by the weak coupling then.

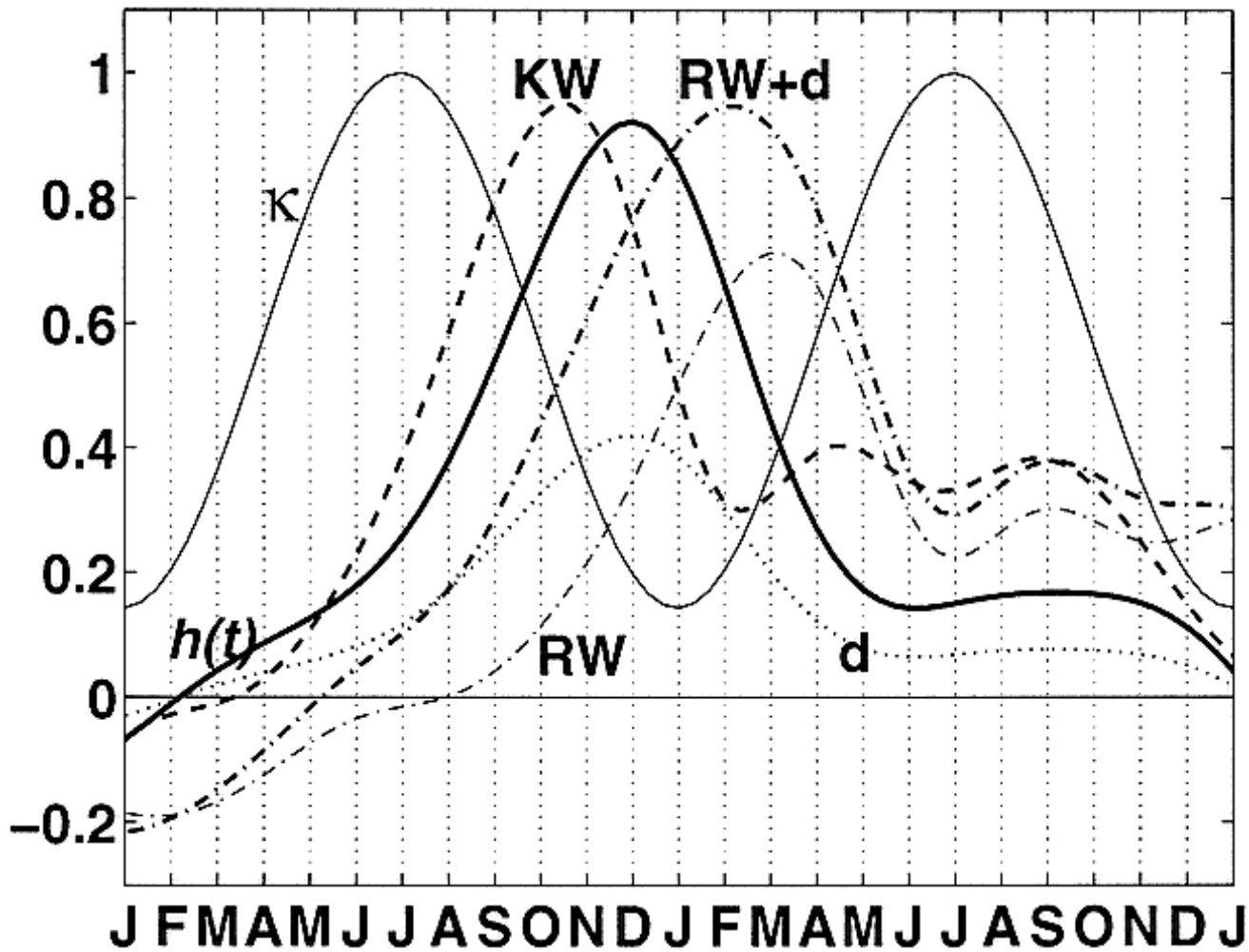

Tziperman et al. 1998

Western Pacific Turnabout

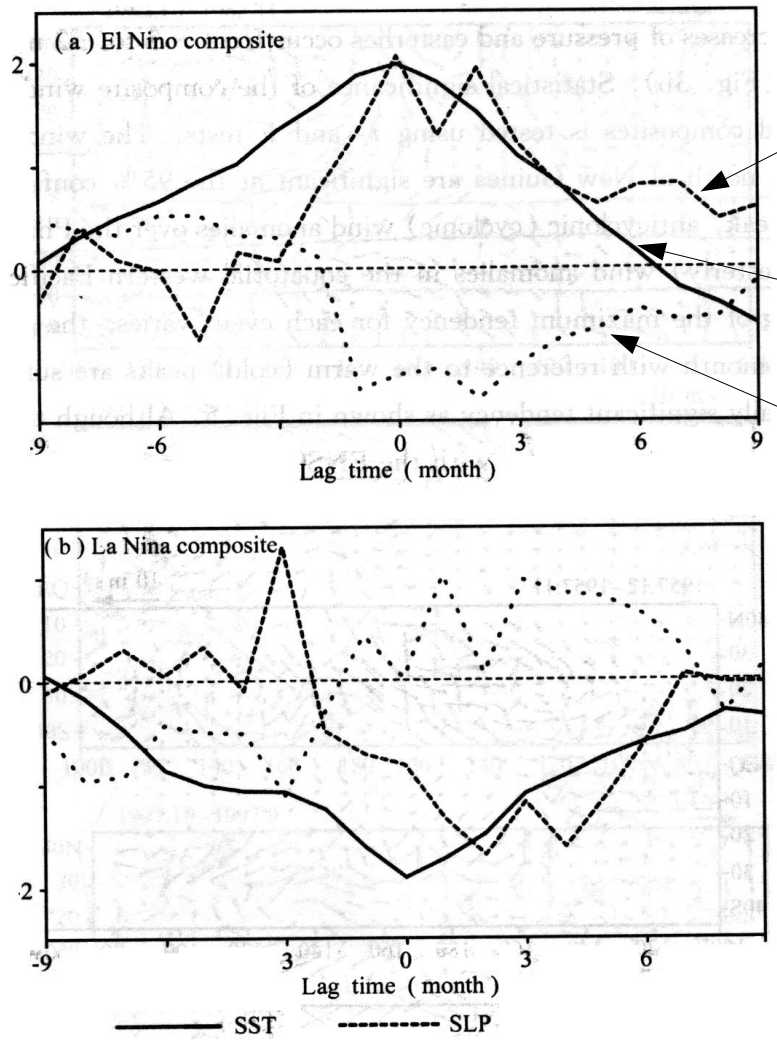

SLP, Phil. Sea

SST, NINO3.4

Wind stress, north of N Guinea

Figure 3 Composite SST anomalies (℃) in Nino3.4 region (solid curves), sea level pressure anomalies (hPa) over the Philippine Sea (dashed curves), and surface zonal wind anomalies (m s^{-1}) north of New Guinea (dotted curves) for the six major warm (a) and the five major cold (b) events on Fig. 2. The composite is made according to the peak warm (cold) months with the abscissa denoting the lag time (month)

Wang, Wu, Lukas, An 2001

ENSO composite 1/2 month prior to peak warming/cooling

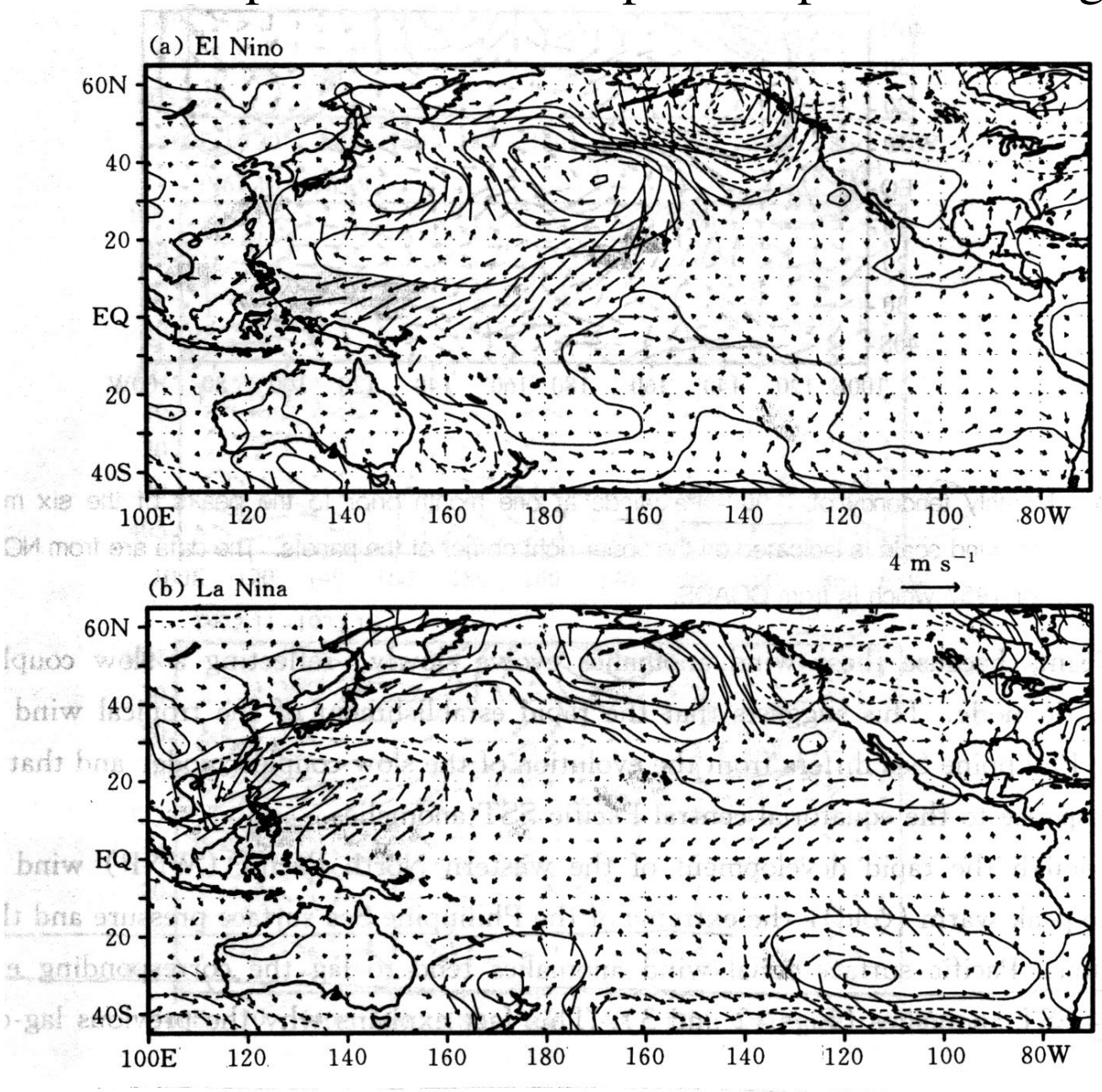

SLP and tau tendency

Wang, Wu, Lukas, An 2001

Rate of change of temperature along equator

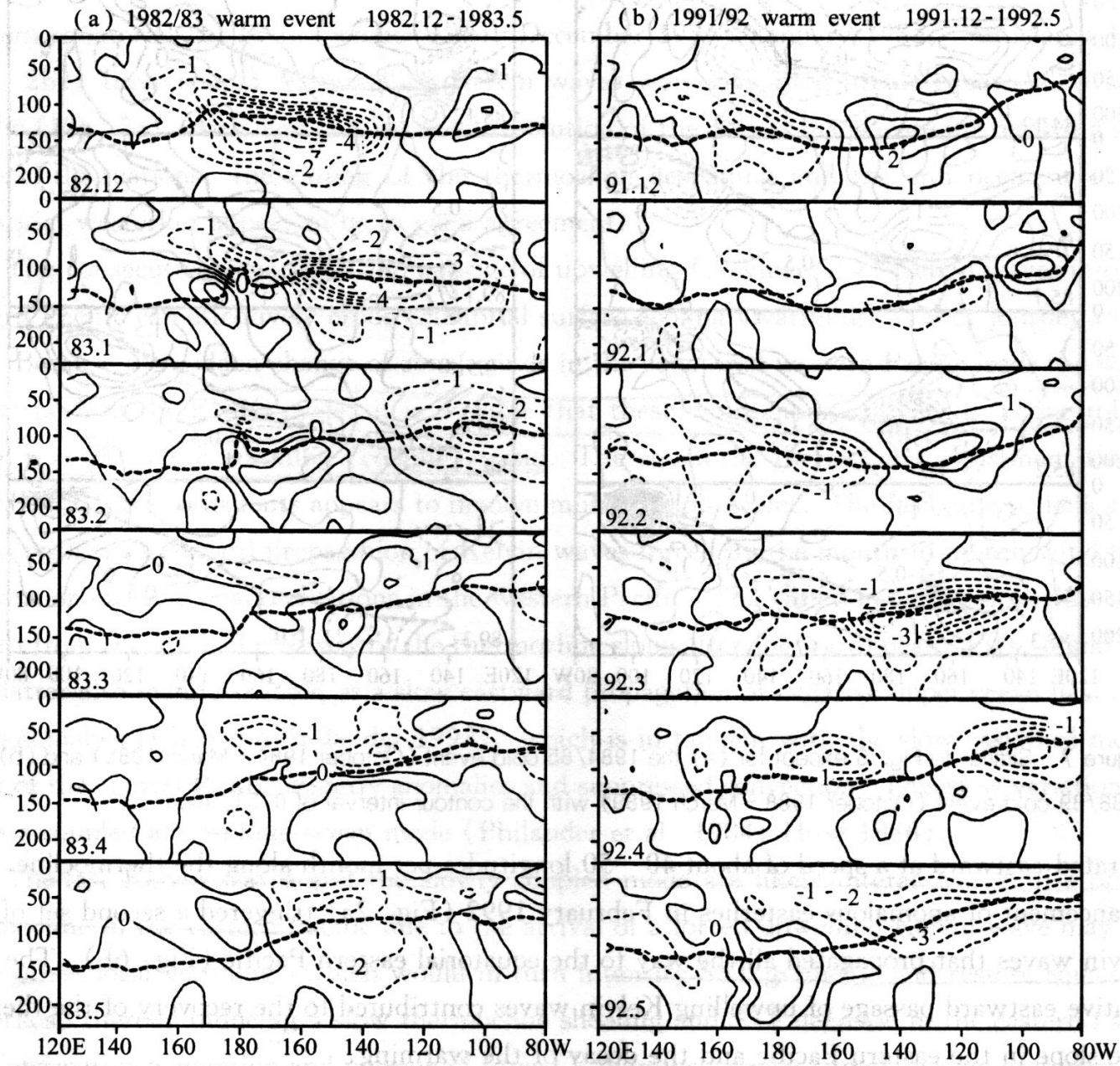

Wang, Wu, Lukas, An

Why does Philip Sea perturbation persist?

3 month prior to peak

Establish SST/SLP anomalies that enhance each other by increased wind speed, only in NE trade season

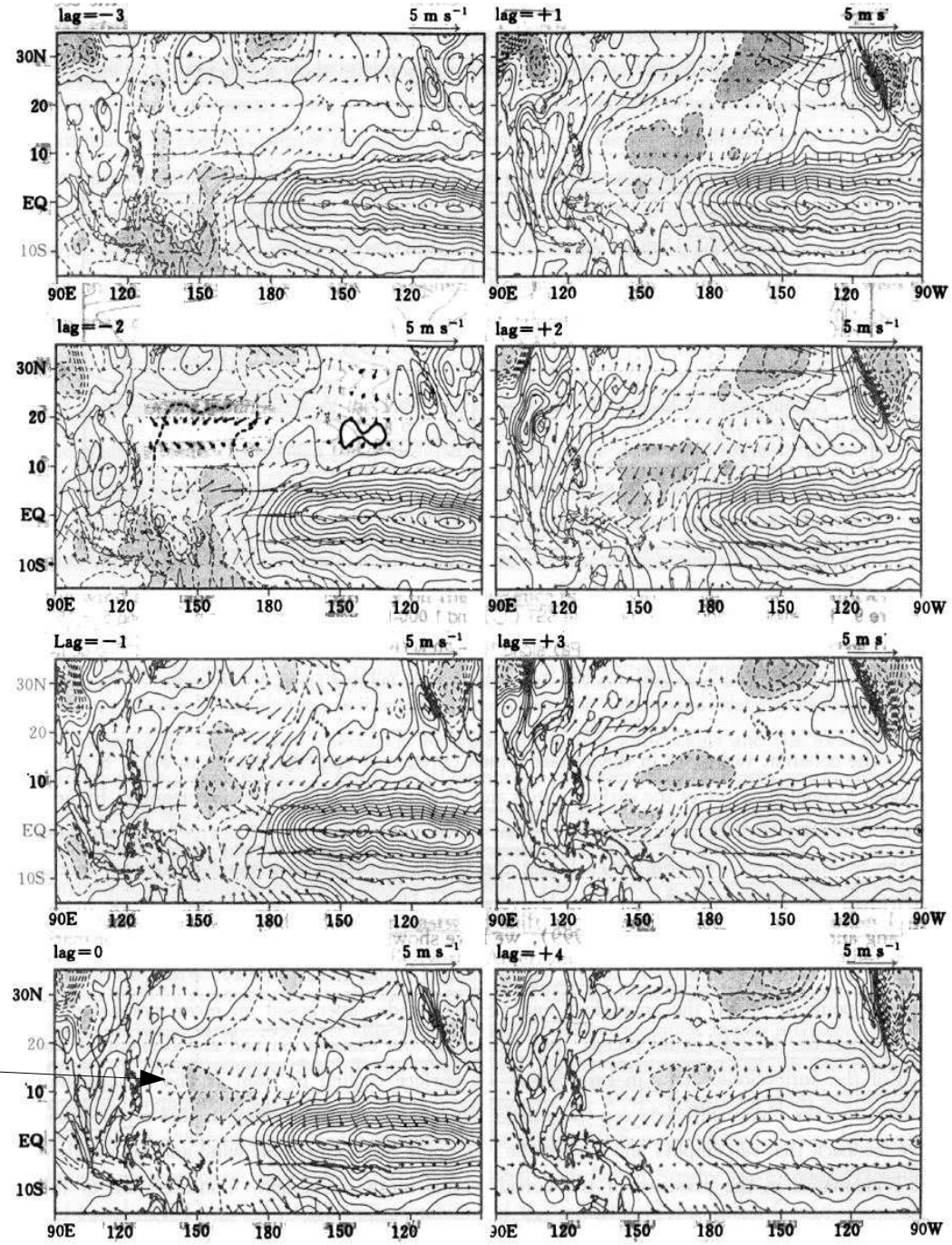

Figure 8 Composite SST and 1 000-hPa wind anomalies during the reversal of the warming trend from 3 months before (lag = −3) to 4 months after (lag = +4) the warm peak. The contour interval is 0.2℃. Shading denotes SST anomalies less than −0.4℃. The wind scale is given at the upper-right corner of the panels.

Wang, Wu, Lukas, An 2001